Modulation of Coherent Microwave Backscatter by Shoaling Waves

W. J. PLANT, W. C. KELLER, AND J. W. WRIGHT

Ocean Sciences Division, Naval Research Laboratory, Washington, D. C. 20375

The orbital speed of long shoaling waves and the modulation of centimetric wind-generated waves by the shoaling waves were obtained from the frequency and amplitude modulations, respectively, of the backscattered signal of a coherent CW 9.375-GHz radar operated from the end of a pier on the Outer Banks of North Carolina. Modulations anomalously large in comparison with those predicted by the relaxation time model (Keller and Wright, 1975) were observed in the range of wind speeds 4.5–6.5 m s^{-1}, which was perhaps coincidentally near the shallow water wave speed. Outside this range of wind speeds the model qualitatively accounted for the magnitude and wind speed dependence of the measured modulations. The phase of the modulation leads to the inference that the maximum amplitude of the short waves occurs near, and generally leeward of, the crests of long waves for wind speeds of up to 8 m s^{-1}, the highest wind speed encountered in the experiment.

1. INTRODUCTION

The short wind-generated waves of the ocean surface are spatially and temporally modulated by longer waves. Remote sensing of ocean waves by microwave radar depends on these modulations [*Wright*, 1977], which may also induce transfer of substantial energy between short and long waves [*Longuet-Higgins*, 1969; *Hasselmann*, 1971; *Valenzeula and Wright*, 1976; *Garrett and Smith*, 1976]. A recent laboratory investigation using microwave scattering [*Keller and Wright*, 1975, 1976] produced a phenomenological theory, the relaxation time model, which accounted for the magnitude, phase, and wind speed dependence of the modulations for winds of up to about 8 m s^{-1} and wave periods as long as 1.75 s. The objective of the experiment reported here was to measure the modulations of short wind-generated waves by waves with typical ocean wave periods and to compare them with predictions of the relaxation time model.

A coherent CW microwave radar such as that used by *Keller and Wright* [1975, 1976] is a self-contained two-scale wave probe. The measure of the larger-scale waves, several meters in length, is the orbital speed, which is obtained from the frequency modulation of the received signal (section 2). At appropriately chosen viewing angles the primary scatterers are short waves a few centimeters in length. Hence the amplitude modulation of the received signal is a measure of the modulation of the small-scale waves. Two sources of modulation of the scattered microwave power have been noted: modulation of the orientation of the small-scale waves, called tilting; modulation of the amplitude of the small-scale waves, exemplified by the straining of the short waves by the horizontal component of the orbital velocity of the large waves.

The horizontal component of the orbital velocity of shoaling waves much exceeds the vertical component except in the region near the wave crests. Hence the relative importance of modulation due to tilting is much reduced over most of the wave so that shoaling waves beyond the surf zone provide perspicuous modulating conditions. Such waves are conveniently observed from sport fishing piers which may be found along many coasts. Records from a wave staff maintained at Jennette's Pier, Nags Head, North Carolina, by the Coastal Engineering Research Center, Fort Belvoir, Virginia, revealed a higher probability of occurrence of large, nearly monochromatic spectral peaks there than at other sites along the Atlantic coast where wave staffs were operated [*Thompson*, 1974]. We therefore chose Jennette's Pier as our experimental site. Bottom profiles were measured along the pier [*Everts and DeWall*, 1976] during the periods when we performed our experiment. The average bottom slope was 0.014 along the seaward two thirds of the pier, which extends 200 m into the Atlantic Ocean. The mean water depth with respect to mean sea level at the end of the pier, where our microwave measurements were made, was 3.5 m during both periods of experimentation, September–October 1975 and April 1976.

The microwave system consisted of a CW transmitter operated at 9.375 GHz and a coherent receiver similar to that described in our previous work [*Wright*, 1966; *Duncan et al.*, 1974], the principal difference being the use of two antennas instead of a single antenna and a circulator. The parabolic antennas were aimed at the same spot on the water surface by adjusting for maximum return. The antennas were about 6 m above the mean water surface at nominal depression angles of 35°. With antenna beam widths of 4° this produced an illuminated spot approximately 2 m long on the water surface. All field data to be reported here were taken when wind and wave directions were within 40° of each other and the antennas were directed toward the incoming waves. Wind speeds were measured by using a Pitot-static tube mounted 7 m above msl and were recorded on one channel of an analog tape recorder; the output of the microwave system was simultaneously recorded on a second channel.

Power spectra and correlations (section 3) were obtained with a Nicolet Scientific Instruments model UA500 spectrum analyzer and model 202C correlator, respectively. Coherences were obtained by using the same manufacturer's model 421A fast Fourier transform analyzer. Both the orbital speed and the modulated backscattered power exhibited nearly monochromatic spectral peaks at the shoaling wave frequency where the coherence between them was greater than 0.8. The measured modulations in these spectral peaks are compared (section 4) with linear monochromatic solutions of the relaxation time model.

2. DETERMINATION OF ORBITAL SPEED FROM MICROWAVE MEASUREMENTS

The Doppler shift of the microwave return gives the mean velocity component along the antenna look direction of the scatterers within the illuminated area. Calling this line-of-sight speed $v(t)$, we have,

$$v(t) = f_D\lambda_0/2 = u \cos\theta + w \sin\theta \quad (1)$$

Copyright © 1978 by the American Geophysical Union.

Paper number 7C0963.
0148-0227/78/037C-0963$03.00

where f_D is the Doppler frequency shift, λ_0 is the microwave length, θ is the depression angle, and u and w are the horizontal and vertical scatterer speeds, respectively. If mean current velocities are small, the principal contribution to u and w will be due to the orbital velocities of long waves which advect the scatterers; smaller contributions due to the intrinsic scatterer velocity and the wind drift at the water surface will also be present. Since the length of the illuminated area is much smaller than the wavelength of any long wave of interest, we may neglect the variation in the orbital velocity over the spot. Then for a sufficiently small monochromatic shallow-water wave we have

$$u = U_0 \cos \Omega t + c_0 + \alpha q$$
$$w = U_0 \tanh Kd \sin \Omega t \left[1 - \left(\frac{c_0 + \alpha q}{C}\right)\right] \quad (2)$$

where c_0 is the intrinsic scatterer speed including any mean current, q is the wind drift, d is the water depth, K is the wave number of the long wave, Ω is its radian frequency, and C is its phase speed. The dimensionless constant α accounts for the fact that the wind drift diminishes rapidly with depth so that its surface value q is not effective in advecting the scatterers. A value $\alpha \doteq 0.7$ has been observed in wave tanks [*Keller et al.*, 1974]. The orbital speed U_0 is related to wave amplitude by the expression

$$U_0 = \Omega A \coth Kd \quad (3)$$

Phillips and Banner [1974] recently showed that the wind drift q is augmented by surface waves, its value being larger near crests. To first order in U_0/C and q_0/C this augmentation is given by

$$q = q_0 + [q_0/(C + q_0)]U_0 \cos \Omega t \quad (4)$$

Substituting (2) and (4) into (1), we find that to first order,

$$v(t) = (c_0 + \alpha q_0) \cos \theta + U_0\{\cos^2 \theta + \sin^2 \theta \tanh^2 Kd + (2/C)[\alpha q_0 \cos^2 \theta - (c_0 + \alpha q_0) \tanh^2 Kd \sin^2 \theta]\}^{1/2} \cos (\Omega t + \phi_D) \quad (5)$$

where

$$\tan \phi_D = \left\{\frac{[1 - (q_0/C)][1 - (c_0 + \alpha q_0/C)]}{1 + (\alpha - 1)q_0/C}\right\} \tanh Kd \tan \theta \quad (6)$$

Thus the component of $v(t)$ at a particular longwave frequency is proportional to the orbital speed of the wave according to (5) and is shifted in phase from the horizontal component of the orbital velocity according to (6).

Keller and Wright [1976] compared microwave measurements of $v(t)$ in a wave tank with values calculated by using (5). Long waves were generated by a plunger, and winds of various speeds were blown across the undulating surface. Wave amplitudes were measured by using a capacitance probe, and orbital speeds were calculated from them by using (3). Winds were given in terms of the air friction velocity u_* determined from measurements of logarithmic velocity profiles and were about one twentieth the midtunnel wind speed. Outputs from the capacitance probe and from the microwave system after frequency-to-voltage conversion were autocorrelated. The amplitudes of the periodic parts of the autocorrelation functions were measured, and from them the amplitude at the fundamental frequency of the long wave was determined. Note that this technique discriminates against even harmonics of the fundamental plunger-generated wave.

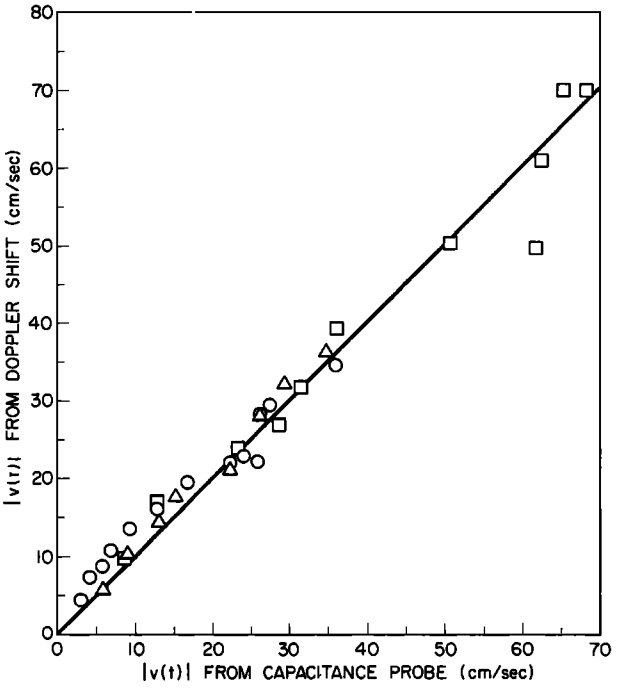

Fig. 1. Line-of-sight speed computed from Doppler shifts compared with that calculated from wave amplitudes. The solid line is theory. Measurements were made in a wind wave tank. Values are as follows: u_* = 16.5 cm/s, f = 0.575 Hz (circles); u_* = 30 cm/s, f = 0.575 Hz (triangles); and u_* = 64 cm/s, f = 0.9 Hz (squares).

Results of this comparison (Figure 1) showed that although the maximum large-wave phase speed was less than 3 m s^{-1}, the error made in ignoring the wind drift and intrinsic scatterer speed in calculating orbital speed from the line-of-sight speed $v(t)$ was 5% or less. No effect of the wind drift or the intrinsic

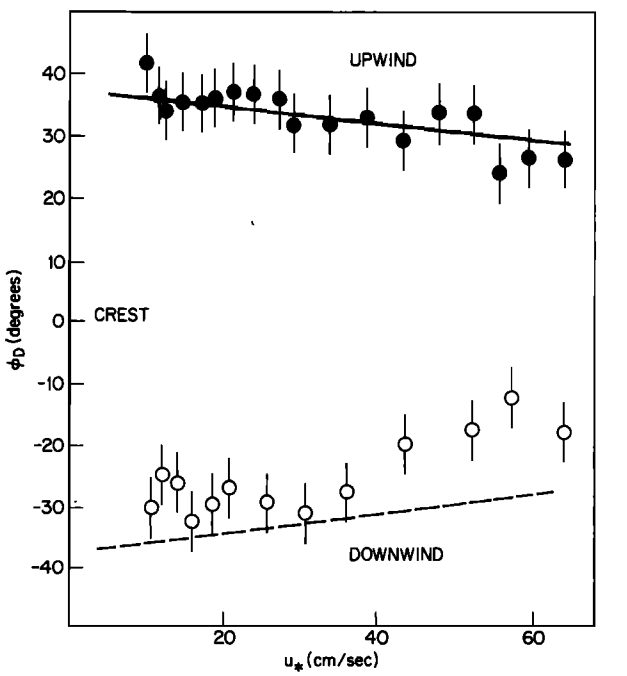

Fig. 2. The phase by which the line-of-sight speed leads the longwave crest. Solid and dashed lines are theoretical. Measurements were made in a wind wave tank. Here f = 0.575 Hz and U_0/C = 0.09.

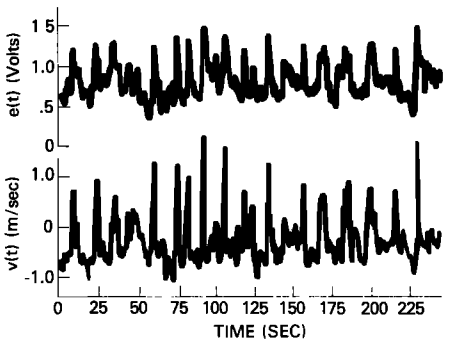

Fig. 3. Processed microwave return from shoaling waves. The top trace is the rectified signal amplitude $e(t)$, while the lower trace is the line-of-sight speed $v(t)$, delayed by 1.25 s from the top trace. Both signals have been low-pass-filtered with a 0.6-Hz cutoff.

scatterer speed was reliably measurable because the error in the capacitance probe calibration was of the same order. A weak wind speed dependence of the phase of $v(t)$ (Figure 2) due to the wind drift was discernible. This phase was measured by cross correlating the frequency-to-voltage-converted microwave output with that of the capacitance probe and was found to be in satisfactory agreement with the phase calculated from (6). The unexplained deviation between measured and calculated phases when looking downwind (Figure 2) was greater in the case of higher modulating wave frequencies but always occurred at wind speeds higher than those prevailing in the experiments reported hereinafter.

3. Spectral Properties of Modulated Backscatter From Shoaling Waves

The ability of the microwave system to measure longwave orbital speeds eliminated the need to perform auxiliary measurements of longwave properties during the modulation experiment. Phase, frequency, and magnitude of the long waves could all be obtained from the orbital speed which was measured simultaneously with, indeed was extracted from, the signal from which the shortwave amplitude modulation was obtained. Wave direction was accurately discernible visually.

The line-of-sight speed $v(t)$ and a rectified scattered field strength $e(t)$, both obtained from the same received microwave signal, are shown in Figure 3. Both channels have been low-pass-filtered with a cutoff frequency of 0.6 Hz. The traces in this figure are synchronized, but the lower trace was delayed by 1.25 s during processing. The spiky nature of these signals results from a succession of narrow wave crests. For such waves the maximum value of $v(t)$ probably leads the wave crests by about 1 s or less for the depression angles used here, the precise time increment being dependent on wave amplitude and water depth. Thus Figure 3 shows that maximum backscattered power occurs very near wave crests.

The power spectra of $e(t)$ or $v(t)$ (Figure 4) show contributions from both the wave crests and the low-amplitude quasi-periodic portions of the wave. We generated power spectra of additional records obtained, first, by clipping the spikes from a wave record and, second, by clipping the underlying portion of the wave record, leaving only the spikes, and compared them with power spectra of the original records. The contribution to the narrow peaks in the clipped spectra of the first type differed from that in the spectra from the original record by less than 25%, which is within the statistical error. The narrow peaks in the clipped spectra of the second type were less than 5% of those in the original spectra.

The relative independence of the two portions of the wave record is presumably the result of the aperiodicity of the crests; the duration of a crest is less than the variation in time between waves (Figure 3). Thus the crests contribute to the autocovariance of $v(t)$ and $e(t)$ (Figure 5) mainly in the region of time lags that are small in comparison with the wave period; for longer time lags the correlations are quasi-periodic. The corresponding narrow spectral peaks in the power spectra (Figure 4) are thus largely attributable to the low-amplitude portions of the wave, while the underlying broad background is due to the wave crests. This dichotomy was exhibited by all of the records used hereinafter. Large breaking waves, notably some of 14-s period resulting from the offshore passage of a hurricane, produced substantial higher harmonic peaks in the

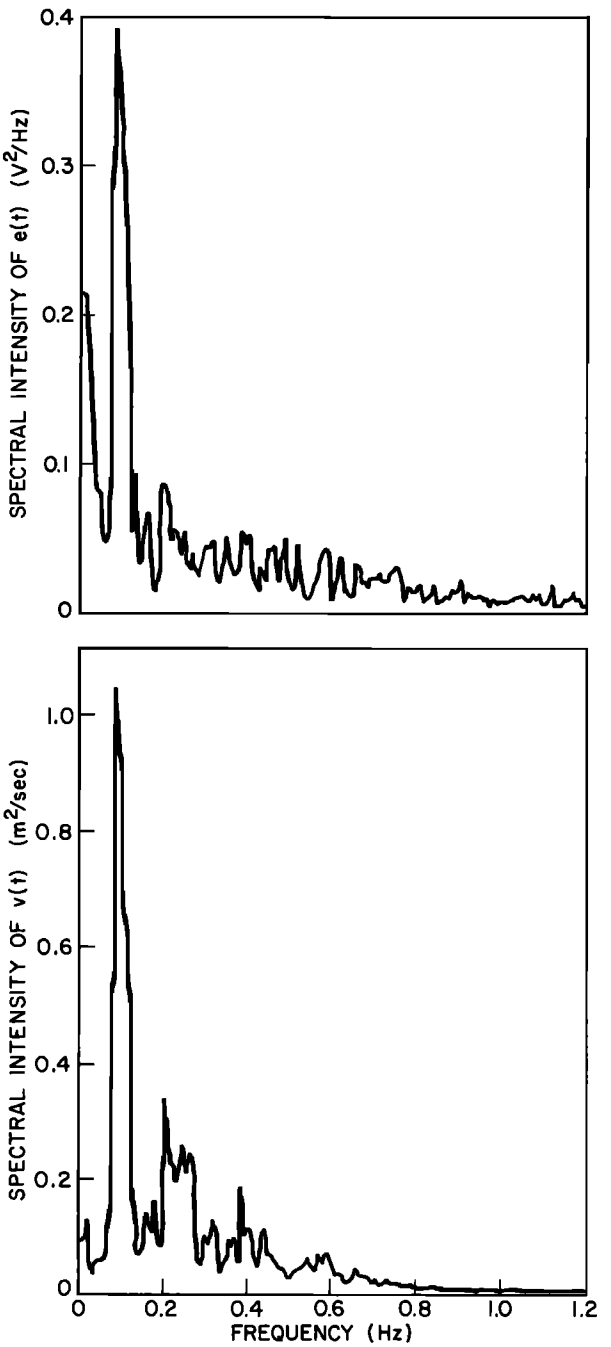

Fig. 4. Power spectra of rectified backscattered signal amplitude $e(t)$ and line-of-sight speed $v(t)$.

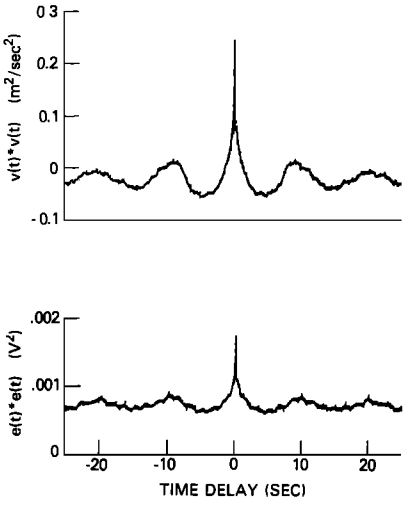

Fig. 5. Autocovariance functions of line-of-sight speed $v(t)$ and rectified backscattered signal amplitude $e(t)$.

power spectra, but such waves are excluded from further consideration here. The effects of breaking per se should be largely confined to the spiky portion of the wave record. A total of 24 records, each of 15-min duration, were analyzed for comparison with theory. These are tabulated (Table 1) in chronological order. Wind and wave directions are those from which the wind and waves approached the pier; 0° indicates north, and 90° is east.

The narrow peaks in the spectra were used to obtain quantitative measurements of the modulation shown in Table 1. The procedure was to integrate over the peak in the $e(t)$ spectrum, divide by $\langle e(t)^2 \rangle$ obtained from the autocorrelation function, and multiply by 2 to yield the fractional modulation M defined by *Keller and Wright* [1975]. Another measure of the modulation is the modulation transfer coefficient m, also defined by *Keller and Wright* [1975]. This quantity, which is simply the mean fractional change in backscattered power, is obtained from M for these data by dividing by 0.35 and taking the square root. The mean-squared orbital speed $U_0^2/2$ of the long wave was measured by integrating over the peak in the $v(t)$ spectrum and dividing by the factor in braces in (5). As was explained in section 2, the terms in (5) containing q_0 and c_0 could be ignored. The line-of-sight speed and the modulation of backscattered power were highly coherent at the spectral peak. Values of $C(f_p)$, the ratio of the square of the cross spectra of $e(t)$ and $v(t)$ to the product of the respective autospectra, evaluated at the spectral peak are given in representative cases in Table 1. The coherence was also moderately high, of the order of 0.4, in the portions of the spectra attributable to the wave crests, but spectral peaks only are utilized here.

The phase of the modulation pattern with respect to the line-of-sight speed was measured by filtering $e(t)$ to pass only signals near the peak frequency and cross-correlating this with $v(t)$. To obtain a correction for phase shifts due to filtering, the filtered $e(t)$ signal was also cross-correlated with the unfiltered $e(t)$. A further correction of $-360(\Omega/8\pi)$, which was always less than 16° in magnitude, was made to account for the lag introduced during frequency-to-voltage conversion. Finally, the phase of $e(t)$ with respect to the horizontal component of orbital speed of the quasi-periodic portion of the wave record was calculated by using ϕ_D as given by (6).

4. Comparison With the Relaxation Time Model

The relaxation time model [*Keller and Wright*, 1975] relates the modulation of backscattered microwave power to the tilting and straining of short waves, in this case, approximately 2-

TABLE 1. Field Data

Wind Speed, m/s	Wind Direction, deg	Wave Direction, deg	f_p, Hz	U_0, cm/s	m	M	φ, deg	Coherence $C(f_p)$
			September 22, 1975					
4.1	95	65	0.10	32	0.27	0.026	+12	
3.7	95	65	0.08	42	0.26	0.024	+10	
3.4	95	65	0.09	36	0.37	0.048	+9	0.9
4.0	95	65	0.10	36	0.29	0.030	+20	
4.1	95	65	0.09	36	0.31	0.034	+26	
			September 25, 1975					
4.8	130	95	0.11	32	0.43	0.066	+4	0.9
			April 19, 1976					
5.1	120	80	0.11	25	0.55	0.106	−2	
6.5	120	80	0.11	42	0.69	0.168	+11	
6.0	120	80	0.10	22	0.60	0.128	+18	
6.3	120	80	0.11	21	0.65	0.150	+7	0.8
5.5	120	85	0.11	32	0.66	0.152	−8	
6.0	120	85	0.10	27	0.58	0.118	−7	0.9
			April 27, 1976					
6.0	15	25	0.15	34	0.60	0.124	+22	
6.5	15	25	0.16	35	0.52	0.096	+33	0.8
6.6	30	20	0.18	32	0.24	0.020	+21	
7.0	30	20	0.14	46	0.29	0.030	+22	0.75
7.4	30	20	0.16	29	0.08	0.002	+30	
7.5	30	20	0.18	34	0.19	0.012	+33	
8.0	30	20	0.15	24	0.13	0.006	+34	0.6
			April 28, 1976					
4.7	40	35	0.18	35	0.50	0.088	−8	
3.8	40	35	0.18	29	0.45	0.072	−3	0.9
3.1	40	35	0.17	41	0.47	0.078	−2	
2.7	40	35	0.15	25	0.25	0.022	−20	
2.4	40	35	0.18	21	0.25	0.022	−1	0.8

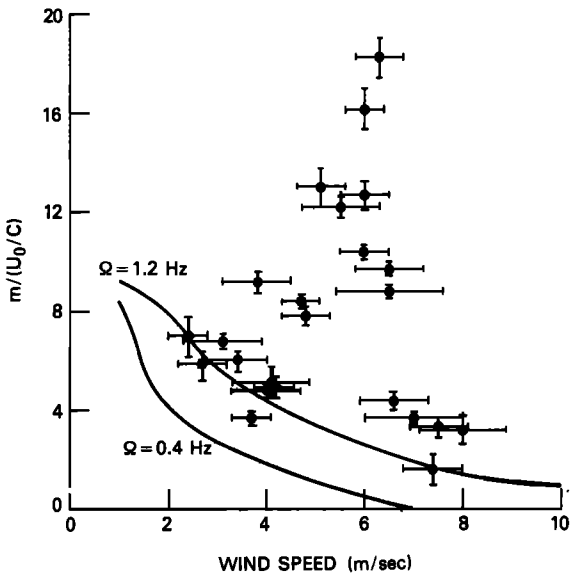

Fig. 6. Modulation transfer coefficient normalized by (U_0/C) as a function of wind speed. Solid curves are predictions of relaxation time theory.

cm waves, by longer waves. The theory postulates that the result of straining is the perturbation of the steady state wind wave spectrum by a longer wave and the subsequent relaxation of the wind waves toward their steady state via wave-wave interactions. As the wind speed increases, coupling of the wind waves to the wind dominates the coupling to the long wave, and modulation due to straining decreases. The modulation of backscattered power is then primarily due to the tilting of the scatterers and is largest where the depression angle is largest. For a sinusoidal long wave this occurs 90° from the wave crest.

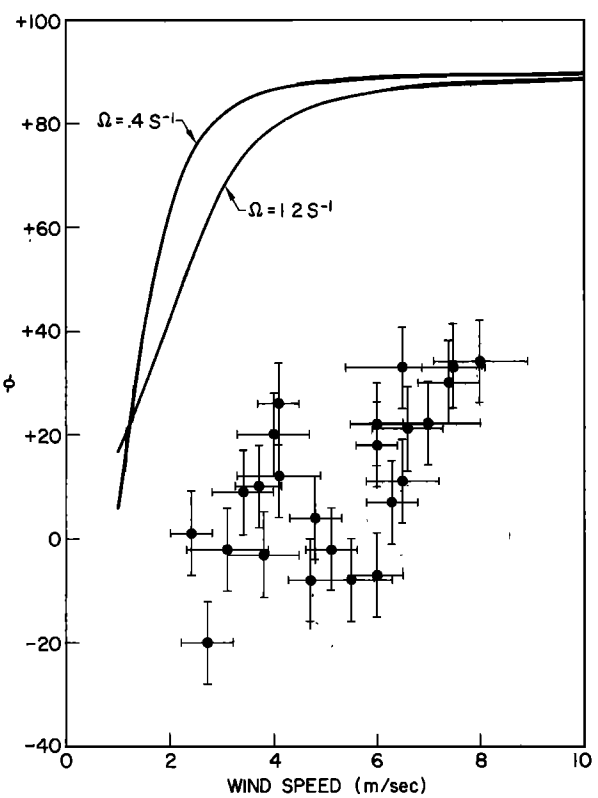

Fig. 7. The phase ϕ by which the quasi-periodic component of the modulated backscattered power leads the corresponding component of the long wave. Solid curves are calculated from relaxation time theory.

The high coherence between the quasi-periodic components of the line-of-sight speed and the modulated backscattered power shows that the two are uniquely related. The regions of the wave near crests, where the rate of strain is high, did not contribute significantly to the quasi-periodic portions of the record. The portions of the wave which do so contribute are the small-amplitude essentially linear regions of the wave where the rate of strain is small. It thus appears sufficiently accurate for our purpose not only to use linear monochromatic solutions to the relaxation problem but to treat the modulating wave as a linear shallow-water wave. Then for the modulation transfer coefficient m we obtain

$$m = (B^2 + D^2 + T^2 - 2DT)(U_0/C) \tag{7}$$

and

$$\tan \phi = (D - T)/B \tag{8}$$

when the wind and waves are in the same direction and the antennas are pointed upwind. In (7) and (8), B and D are the components of straining in and out of phase with the long wave, respectively, and are given for our conditions by

$$B = -\frac{k}{F_0}\frac{\partial F_0}{\partial k} \Big/ \left[1 + \left(\frac{\beta_r}{\Omega}\right)^2\right]$$
$$D = \left(\frac{\beta_r}{\Omega}\right)\left(\frac{k}{F_0}\frac{\partial F_0}{\partial k}\right) \Big/ \left[1 + \left(\frac{\beta_r}{\Omega}\right)^2\right] \tag{9}$$

where $F_0(k)$ is the steady state wind wave spectrum and β_r is a relaxation rate. Similarly, T is the (quadrature) tilt component and is given by

$$T = \tanh Kd \left[\frac{1}{G}\frac{\partial G}{\partial \theta} - \tan\theta\left(\frac{k}{F_0}\frac{\partial F_0}{\partial k}\right)\right] \tag{10}$$

where $G(\theta)$ is a function of scattering parameters [*Wright*, 1966].

We computed theoretical curves for $m/(U_0/C)$ and ϕ in the same manner as Keller and Wright for comparison with the data (Figures 6 and 7). The value of the wave speed C(= 5.9 m s^{-1}), corresponding to the mean depth of 3.5 m, was used in computing values of U_0/C. Relaxation times were taken to be twice the initial growth rates of 2-cm waves measured in our wave tank [*Larson and Wright*, 1975]. For a given value of the parameter $(k/F_0)(\partial F_0/\partial k)$ the maximum value of the modulation given by (7) and (9) occurs for a vanishing relaxation rate. Thus the resonancelike dependence of $m/(U_0/C)$ on wind speed in the range 4.5–6.5 m/s is predictable from (7) and (9) only on the basis of an implausible wind speed dependence of $(k/F_0)(\partial F_0/\partial k)$. The magnitude of the modulation at the lowest and the highest wind encountered in the experiments is predictable from the model if minor adjustments in the value of the relaxation rate are made. The phase of the modulation increases with wind speed but remains within 40° of the crests. Thus the phase has the proper dependence on wind speed but is substantially smaller than that predicted by the model, as was also observed in wave tank measurements [*Keller and Wright*, 1975, 1976]. This discrepancy would have to be accounted for in the model by a source of modulation, the phase of which is different from that of straining. The anomalously large modulation occurs at a wind speed which is, perhaps only coincidentally, nearly equal to the estimated shallow-water wave speed. Note that the dip in the measured phase versus wind speed (Figure 7) occurs in the same restricted range of winds as the anomalously large modulation.

REFERENCES

Duncan, J. R., W. C. Keller, and J. W. Wright, Fetch and wind speed dependence of Doppler spectra, *Radio Sci., 9,* 809–819, 1974.

Everts, C. H., and E. E. DeWall, Coastal sand level changes in North Carolina, report, Coastal Eng. Res. Center, Ft. Belvoir, Va., 1976.

Garrett, C., and J. Smith, On the interaction between long and short surface waves, *J. Phys. Oceanogr., 6,* 925–930, 1976.

Hasselmann, K., On the mass and momentum transfer between short gravity waves and larger scale motions, *J. Fluid Mech., 50,* 189–205, 1971.

Keller, W. C., and J. W. Wright, Microwave scattering and the straining of wind-generated waves, *Radio Sci., 10,* 139–147, 1975.

Keller, W. C., and J. W. Wright, Modulation of microwave backscatter by gravity waves in a wavetank, *Rep. 7968,* pp. 1–21, Naval Res. Lab., Washington, D. C., 1976.

Keller, W. C., T. R. Larson, and J. W. Wright, Mean speeds of wind waves at short fetch, *Radio Sci., 9,* 1091–1100, 1974.

Larson, T. R., and J. W. Wright, Wind generated gravity-capillary waves: Laboratory measurements of temporal growth rates using microwave backscatter, *J. Fluid Mech., 70,* 417–436, 1975.

Longuet-Higgins, M. S., A non-linear mechanism for the generation of sea waves, *Proc. Roy. Soc., Ser. A, 311,* 371–380, 1969.

Phillips, O. M., and M. L. Banner, Wave breaking in the presence of wind drift and swell, *J. Fluid Mech., 65,* 647–657, 1974.

Thompson, E. F., Results from the CERC wave measurement program, in *Proceedings of the International Symposium on Ocean Wave Measurement and Analysis,* vol. 1, pp. 836–855, American Society of Civil Engineers, New York, 1974.

Valenzuela, G. R., and J. Wright, The growth of waves by modulated wind stress, *J. Geophys. Res., 81,* 5795–5796, 1976.

Wright, J. W., Backscattering from capillary waves with application to sea clutter, *IEEE Trans. Antennas Propagat., AP-14,* 749–754, 1966.

Wright, J. W., Detection of ocean waves by microwave radar: The modulation of short gravity-capillary waves, *Boundary Layer Meteorol., 13,* 83–101, 1977.

(Received March 17, 1977;
revised October 6, 1977;
accepted October 17, 1977.)